

Image Compression Exploration using Discrete Wavelets Transform Families and Level

Arbab Waseem Abbas^{1,3}, Waseem Ullah Khan^{2,3}, Safdar Nawaz Khan Marwat^{2,3}, Salman Ahmed^{2,3}, Khalid Saeed⁴, Noor ul Arfeen¹

¹Institute of Computer Science and Information Technology, Faculty of Management and Computer Sciences, The University of Agriculture, Peshawar, 25000, Pakistan.

²Department of Computer Systems Engineering, Faculty of Electrical and Computer Engineering, University of Engineering and Technology, Peshawar, 25000, Pakistan.

³Secured IoT Devices Lab, Department of Computer Systems Engineering, University of Engineering and Technology, Peshawar, 25000, Pakistan.

⁴Department of Computer Science, Shaheed Benazir Bhutto University, Sheringal, Upper Dir, 18200, Pakistan.

* **Correspondence:** Waseem Ullah Khan, waseem@uetpeshawar.edu.pk

Citation | Abbas. A. W, Khan. W. U, Marwat S. N. K, Ahmed. S, Saeed. K, Arfeen. N, "Image Compression Exploration using Discrete Wavelets Transform Families and Level", IJIST, Vol. 6 Issue. 2 pp 366-379, April 2024

Received | Mar 21, 2024, **Revised |** April 15, 2024, **Accepted |** April 18, 2024, **Published |** April 23, 2024.

This analysis paper is based on Discrete Wavelets Transform (DWT) for image compression using wavelets families and levels. The DW transforms the image or data into frequency components that match its resolution scale while the compression removes duplication and unwanted information on the receiver side. Wavelets in compression observe the whole image very finely and thus produce no blocking artifacts. Thus, wavelets are high-quality image compression used in many real-world applications i.e. image, multimedia, biometric and biological analysis, computer graphics and image processing, etc. In this investigation, first of all, various compression methods have been compared. It is validated based on compression ratio that DWT is the optimal choice. Secondly, for experimental and analysis purposes, random real-time digital images both RGB and greyscale have been used as a dataset. The assessment images have been converted to grayscale if RGB, decomposed using wavelet levels, and compressed using wavelet families. Threshold coefficients have been evaluated by the Birge-Massart strategy using two scenarios i.e. simulator control thresholding and increasing threshold. Birge-Massart thresholding is best for the compression of still images in wavelet transform. The evaluation and comparison of various wavelet families and decomposition levels were conducted based on criteria such as image compression effectiveness, retained energy, and zero coefficients. The size of original, compressed, and decompressed images has also been computed and displayed for analysis purposes. The analysis of wavelet families and decomposition levels indicated that increasing levels up to a certain range for decomposition purposes in various wavelet compression families enhances image smoothness consistently. With image smoothness, roughness, and noise spikes in images have been reduced. However, it is observed that after specific levels, image quality degradation has been observed. The significance and novelty of the work provide analysis for appropriate and effective quality image compression using DWT families and levels in different applications. The purpose is to reduce need-based storage requirements and lightweight transmission. Additionally, the optimum compression algorithm in DWT families and levels is also found based on the results. As selection of wavelet filters and decomposition level play an important role in achieving an effective compression performance because no filter performs the best for all images.

Keywords: Image Compression; Discrete Wavelets Transform (DWT); Wavelet Families; Decomposition Levels and Compression Ratio



Introduction:

In industrial and scientific applications, digital imaging has a massive influence, necessitating efficient digital image handling, transmission, and storage of digital images due to bandwidth and storage limitations [1]. Wavelets have vast applications in digital imaging including edge and corner detection, pattern recognition, filter design, and analysis of ECG [2]. Specifically, in image compression, the remarkable application of wavelet is JPEG2000 which achieves high accuracy with no blocking effect [3]. Wavelet decomposition allows for image decomposition based on resolution levels and sequential processing from low to high resolution. This is because wavelets exhibit localization in both spatial (time) and frequency domains.

HAAR is the simplest and oldest wavelet, daubechies are the foundational in wavelet theory and are popularly used in signal processing and many other applications. The orthogonal wavelets are strongly supported by HAAR, Symlets Daubechies, and Coiflets. These wavelets are suitable for reconstruction along with Meyer wavelets. The symmetric shape wavelets are Meyer, Mexican Hat, and Morlet. The HAAR, known for their simplicity and discontinuous nature, are the oldest wavelets. Wavelets are selected for particular applications on the basis of their shape and ability to analyze the signal [4].

The wavelets transform offers the simultaneous analysis of both frequency and time analysis. It therefore plays a vital role in image compression [5]. Compared to the Fourier transform, the wavelets transform is preferred for image compression applications as mentioned in [6]. Wavelets transform excels in the computation of spectral information because it operates on localized segments of the signal, unlike the Fourier transform, which requires information about the entire signal over the entire time domain. This localized processing makes wavelet transform more practical and efficient for tasks like image compression where only specific parts of the signal need to be analyzed and transformed [7].

The research conducted in [8] offers a comparison and analysis of various wavelet-based techniques including DWT, Continuous Wavelet Transform (CWT), Fast Wavelet Transform (FWT), and Wavelet Packets. In [9], an algorithm is proposed for image compression based on the Antonini 7/9 wavelet filter, which consists of wavelets transformed in order to separate the image into sub-bands, followed by the coefficient's quantization. The distortion is minimized by using an error metric, which approximates the reconstituted coefficients quantization error. Experimental results revealed that in comparison to jpeg compression, the proposed algorithm is efficient and produces a reconstructed image of better quality. The authors in [10] highlight the importance of compressed images for industrial and scientific applications due to the high bandwidth and storage requirement for uncompressed images. Experimental results indicate improved efficiency and quality compared to JPEG compression. In [11], modified DWT is presented for edge detection of noisy medical images, which detects edges at every resolution and morphological thinner, which connects all information containing edge points and disconnects unwanted edge points.

In [12], Edge-based Transformation and Entropy Coding (E/TEC) algorithms have been proposed for the compression of pixelated images, which are commonly utilized for the transmission of data between digital devices that have screens and cameras. In [13], the authors proposed a scheme for compression and optimization of an image using DWT and evolutionary algorithms including artificial bee colony and particle swarm optimization for best-quality images respectively. The authors in [14] discussed an approach of Haar wavelet transform, run length encoding, and Discrete Cosine Transform (DCT) procedures for progressive industrial methods with high image compression requirements. These procedures convert an image or signal into half of its length called "detail levels" and then the compression procedure is completed. In [15], authors improved the DWT-based JP3D compression of volumetric medical images. They applied new approaches formerly used in 2D image compression i.e. reversible denoising and

lifting steps with step skipping and a hybrid transform combining 3D-DWT with prediction [16].

The author in [17] highlights the advantages of the DWT-based image compression method by utilizing the canonical Huffman coding as an entropy encoder. In [18], authors presented the utilization of HAAR wavelet-based DWT for effective and efficient image compression. Moreover, in [19], an analysis of the most common techniques in image compression is presented. Various state-of-the-art lossless image compression algorithms i.e. run-length, entropy, and dictionary-based algorithms were compared on various bench-marked images. In [20], the most advanced lossless image compression algorithms including JPEG, JPEG 2000, and PNG, focus on the strength of each algorithm for different kinds of images using more than one parameter. In [21], an approach of Haar wavelet transform, discrete cosine transforms, and run length encoding techniques for advanced manufacturing processes with high image compression rates are presented.

Objective and Novelty:

Due to the pragmatism of the transformation of wavelet, this research work is engraved for investigation and improvements of wavelet transformation through observation of wavelet decomposition levels and wavelet families. The significance and novelty of the work provide analysis for appropriate and effective quality image compression using DWT families and levels in different applications. The purpose is to reduce need-based storage requirements and lightweight transmission. Additionally, the optimum compression algorithm in DWT families and levels is also found based on the results. As selection of wavelet filters and decomposition level play an important role in achieving an effective compression performance because no filter performs the best for all images.

Compression Methods Comparison:

The analysis presented in Table 1 of this research paper compares various widely used image compression formats based on the compression ratio for images. The GIF, PNG, JPEG, DCT, and DWT-based image compression formats are described by [22], wherein DWT provides the best results in terms of high compression ratio, lossless compression, and improved image quality. Therefore, it is justified that DWT is an appropriate choice for image compression. We analyzed DWT in terms of compression levels and decomposition families.

Table 1: Compression Methods Comparison

Presentation	Designation	Ratio of Compression	Explanation
GIF	Graphics Interchange Format	4:1-10:1	Lossless for flat color-edged art or text
PNG	Portable Network Graphics	10-30% smaller than GIFs	Lossless for flat-color, sharp-edged art
JPEG	Joint Photographic Experts Group	10:1-100:1	Best suited for continuous-tone Images
DWT	Discrete Wavelet Transform	30-300% greater than JPEG, or 600:1 in general	High compression ratio, better image quality without much loss
DCT	Discrete Cosine Transform	1:6 in DCT VS 1:9 in DWT	Comparatively less compression ratio, low quality, and much less than DWT

Material and Methods:

Image compression based on transformation schemes consists of three steps; firstly, it transforms spatial domain image into another domain. Compression is the second step where the transformed image is quantized i.e., data samples with insignificant energy are discarded. The

third step is inverse transformation which reconstructs the compressed image in the spatial domain. Figure 1 shows a block diagram of the general image compression scheme.

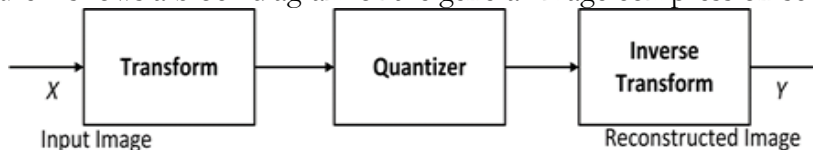


Figure 1: Image compression scheme.

In the general image compression model, the first step is the transformation scheme, which can be DWT, DCT, or JPEG. In the next step, quantization is done. Finally, the image is reconstructed in the inverse transform to see the quality and compression of the image. The DWT can be expressed as:

$$DWT(m, k) = \frac{1}{a} \sum_{n=0}^{N-1} s(n)g\left(\frac{k-b}{a}\right) \tag{1}$$

In Equation 1, a is scalar, b is time, s(n) is the original signal, N is the number of samples in the signal window, g () is a function called mother wavelet, and m is a DL index. DWT is a multi-stage filter. The decomposition of wavelet comprised of filters having two types, i.e. low pass filter as well as high pass filter. In decomposition, the DWT image is split into several sub-bands i.e., LL, LH, HL, and HH; only LL (low-level) sub-band is further decomposed as it has low frequency and noise compared to other sub-band levels. The feature of the overall original image is shown by the LL subband. The image's Vertical features are represented by the LH subband. Horizontal information of the image is denoted by HL while diagonal information is given in the HH sub-band [23] as shown in Figure 2.

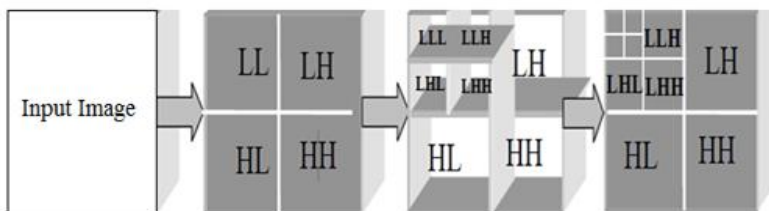


Figure 2: DWT image decomposition levels.

Generally, wavelets-based image compression consists of the following steps as reflected in Figure 3.

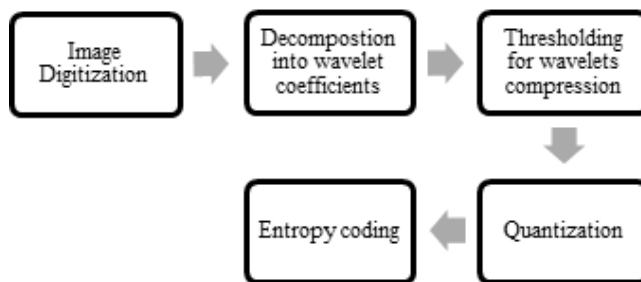


Figure 3: Steps of wavelets image compression.

After converting the image into digital form, the image is decomposed using the proposed DWT algorithm. Afterwards image is compressed by DW transform while for lossless compression thresholding, quantization and entropy coding are used. The implementation steps of 2D wavelets for the devised algorithm are shown in Figure 4.

Birge–Massart thresholding strategy is built-in thresholding in MATLAB for image compression. It is best for the compression of still images in wavelet transform comprising the extent to which the quality of the image is degraded throughout compression as well as decompression. In this research, the following wavelet families i.e., Daubechies, Haar, Symlets,

Coiflets, Bior Splines, Reverse Bior, DMeyer, and decomposition levels up to 8 are utilized for analysis. The DWT families and their representation are shown in Table 2.

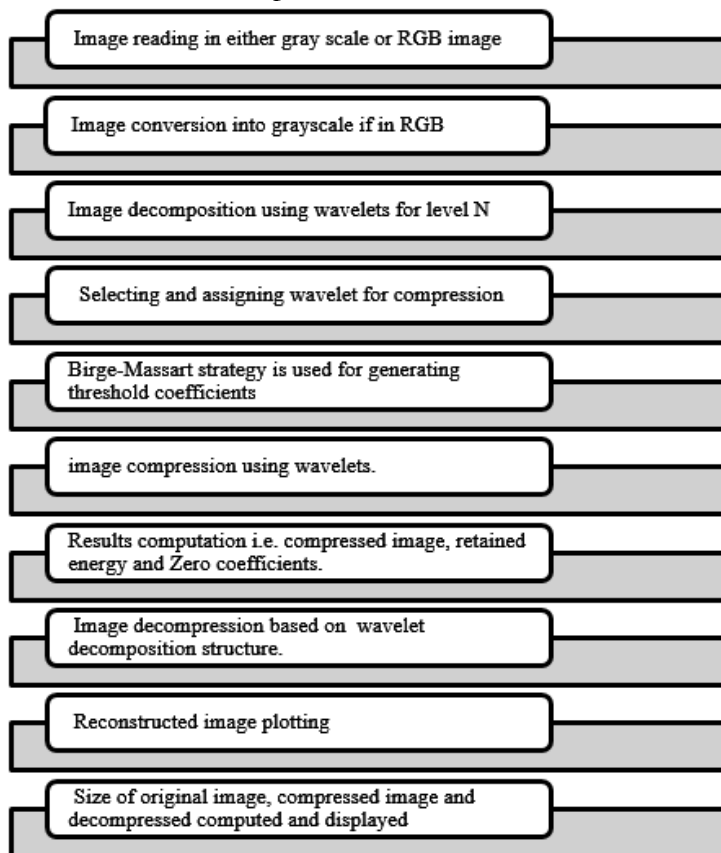


Figure 4: Implementation steps of 2D wavelets.

Table 2: DWT Families

S. No.	Wavelet Families	Representation	Wavelet Families in Each
1	Daubechies	Db	db1 db2 db3 db4 db5 db6 db7 db8 db9 db10
2	Haar	Haar	1
3	Symlets	Sym	sym2 sym3 sym4 sym5 sym6 sym7 sym8
4	Coiflets	Coif	coif1 coif2 coif3 coif4 coif5
5	Bior Splines	Bior	bior1.1 bior1.3 bior1.5 bior2.2 bior2.4 bior2.6 bior2.8 bior3.1 bior3.3 bior3.5 bior3.7 bior3.9 bior4.4 bior5.5 bior6.8
6	Reverse Bior	Rbio	rbio1.1 rbio1.3 rbio1.5 rbio2.2 rbio2.4 rbio2.6 rbio2.8 rbio3.1 rbio3.3 rbio3.5 rbio3.7 rbio3.9 rbio4.4 rbio5.5 rbio6.8
7	DMeyer	Dmey	1

The results of this study are evaluated using families and decomposition levels of DWT, which are applied to grey level and RGB images for analysis purposes. For grey-level image compression, the following steps are applied in the proposed algorithm.

- Take any grey-level image i.e. ('cb.tif')
- Give the decomposition level i.e. 5
- Give the name of the wavelet i.e. ('db4')

- The resultant Compression Ratio percentage/retained energy is 99.3021 as shown in Figure 5

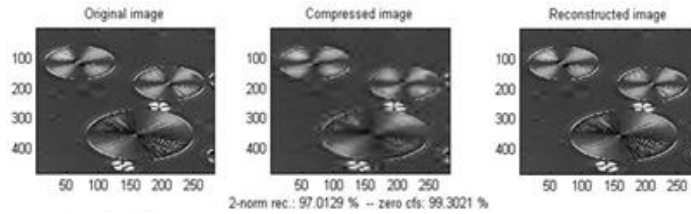


Figure 5: Grey-level image analysis.

For RGB image compression following steps are applied in the proposed algorithm.

- Select any RGB image i.e. ('p1.tif')
- Convert this image to the grey level
- Give the decomposition level i.e. 3
- Give the name of the wavelet i.e. ('db3')
- The compression ratio is 94.7470 as shown in Figure 6

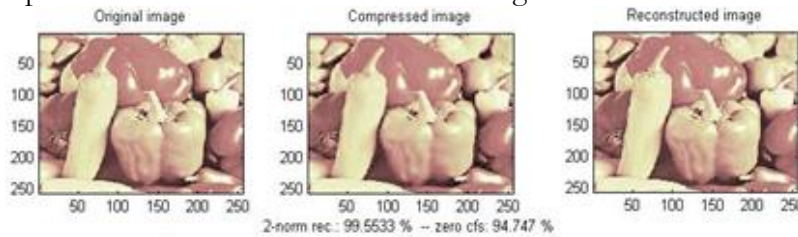


Figure 6: RGB image analysis.

Note that any decomposition level and wavelet family can be used for grey level and RGB image in the proposed algorithm for computation. While equations 2, 3, and 4 are used for compression ratio, retained energy, and number of zeroes.

Mathematically compression is computed as

$$Compression\ ratio = 100 - \left(\frac{1}{ratio} * 100\right) \% \tag{2}$$

Equation 2 has produced the percentage of the original as required. As the results are in percentage therefore inverse of the ratio is multiplied by 100 to get the compression ratio in percentage. For example, if the ratio is 8, take 1/8 give 0.125, and multiply by 100 to get 12.5% of the original. And then subtract from 100 to compute that compression is done by 87.5%. This compression ratio is determined based on DWT analysis i.e. threshold value, retained energy, and number of zeros present in the image after compression as shown in Figure 5 and Figure 6 using Equations 3, 4, and 6. Retain Energy (RE) and Number of Zeros (NoZ) are calculated mathematically

$$RE = \left(\frac{\|Ct\|^2}{\|C\|^2}\right) * 100 \tag{3}$$

where $\|Ct\|$ is the norm of the compressed wavelet coefficients vector and $\|C\|$ is the original image wavelet coefficient vector. Similarly,

$$NoZ = \left(\frac{100 * CDZ}{NC}\right) \tag{4}$$

Scenario 1: This scenario has a simulator control threshold. In scenario 1, different patterns of retained energy in wavelet families at various decomposition levels have been perceived.

Scenario 2: It has an increasing threshold with increasing decomposition levels of DWT.

Results of Wavelets Decomposition:

In Figure 7, the image undergoes decomposition using wavelet levels to achieve various levels of detail. The decomposition of the image was manipulated using low pass filter $g(x)$ as well as high pass filter $h(x)$ by DWT. The complete information shown by the LL portion is $g(x)$

whereas $h(x)$ consists of the LH, HL, and HH subbands of the image. In DWT, the best recognition was achieved at the LL portion as compared to LH, HL, and HH. Therefore, the results were checked with three decomposition levels of DWT at the LL sub-portion having 12 sub-band images and reflected pictorially in Figure 7.

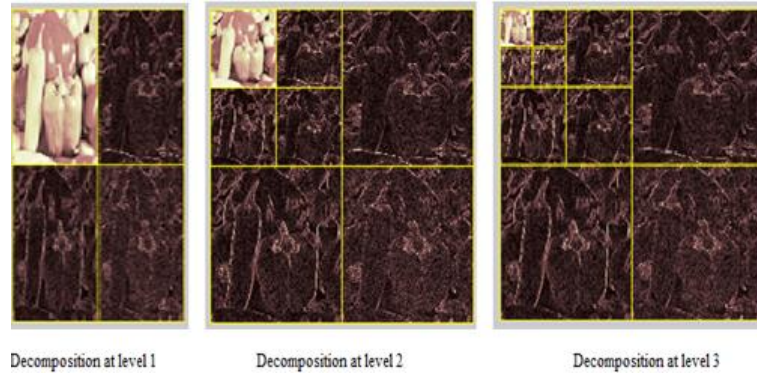


Figure 7: Wavelets decomposition levels.

Analysis of Wavelets Families and Decomposition Levels:

For analysis of an image, Daubechies, Haar, Symlets, Coiflets, BiorSplines, ReverseBior, DMeyer wavelets families, and decomposition levels up to 8 were utilized. The proposed implementation steps of Figure 4 (Implementation steps of 2D wavelets) are evaluated for image compression results analysis. The decomposition levels provide a coefficient matrix for compression purposes. The decomposition level divides the image into sub-bands. Mathematically

$$sb = 4dl \tag{5}$$

Where sb = sub-bands in image, and dl = decomposition level from 8 levels of decomposition, 32 sub-band images are obtained from equation 5. As each decomposition level has 4 sub-band images as shown in Figure 7. This includes the approximation details, horizontal details, vertical details, and diagonal details. After image decomposition, the coefficient matrix is obtained. Subsequently, hard thresholding is performed using the threshold by Birge–Massart strategy. With the hard thresholding, all the coefficients value less than the threshold are discarded and only values equal to or greater than the threshold are kept. Compressed images are reconstructed from the thresholded coefficient values of the image. The compressed image is obtained with the Birge–Massart strategy of thresholding and is analyzed with various decomposition levels and DWT families. This strategy works on the following wavelet selection rule which is given below:

$$LC = \frac{m}{(dl_n+1-dl)\alpha} \tag{6}$$

Let dl_0 = the decomposition level, m = length of the coarsest approximation over 2, and α = real value preferably equal to 1 in our proposed scenario, we have two possibilities i.e. (a) At level $dl_0 + 1$ (coarser level), everything is kept while (b) For level dl from 1 to dl_0 the LC larger coefficients are kept only with the proposed Equation 4. The final results are assessed based on two key criteria including retained energy and thresholding using Equation 3 and 6 respectively. If the retained energy i.e., the amount of energy of an image retained after compression [24], where 100% retention indicates lossless compression, ensuring accurate reconstruction of the image. Conversely, if the retained energy is less than 100%, the compression is considered slightly lossy. The retained energy of various wavelet families is analyzed concerning decomposition levels and thresholds.

Two scenarios have been considered. In scenario 1, the threshold has been taken automatically by the simulator relative to decomposition levels and families of DWT. In scenario 2, the threshold has been increasing for analysis purposes with increasing levels of

decomposition. The thresholding is performed using the threshold by Birge– Massart strategy. The results are discussed in the following sections.

Results on Daubechies DWT Family:

The Daubechies wavelet family is known for its basic and compact nature that encompasses wavelets numbered from db1 to db10. The result analysis using wavelets levels of decomposition up to 8 and Daubechies (*db1*) family are elaborated. In scenario 1 based on the automatic simulator control threshold, when the family is *db1* and the level is rising from 1 to 3, retained energy was reduced up to 97.92% at level 3. Subsequently, from decomposition levels 4 to 8, the random behavior of retained energy after compression is shown in Figure 8. This validates the behavior of Daubechies wavelet filters which are designed with extreme phase and the highest number of vanishing moments for a given support width. Daubechies wavelets are generally used for solving fractal problems, signal discontinuities, etc. While in scenario 2, the retained energy was decreased with changing levels and thresholds.

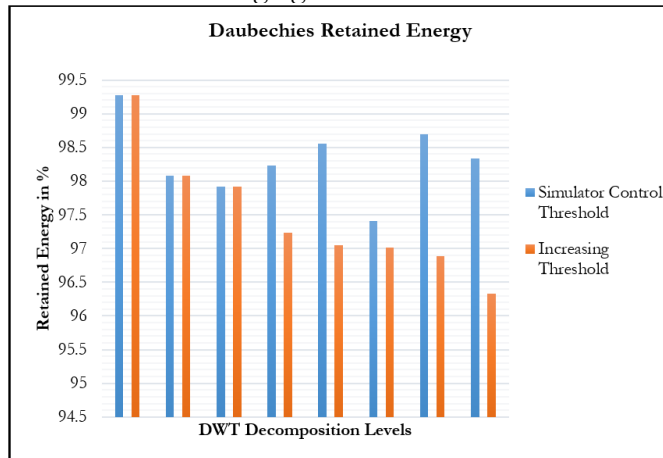


Figure 8: Trend of Daubechies retained energy.

Results on Haar DWT Family:

The Haar wavelet is the simplest form of the wavelets and it uses the step function to approximate the original image. Haar is simple, fast, and memory efficient. The results in scenario 1 using wavelets levels of decomposition up to 8 through the Haar family are shown in Figure 9. In scenario 1, level 3 shows a low retained energy result of 97.92 in percentage while the best result is at level 1 i.e. 99.27%. This decreasing and random pattern of retained energy was due to the nature of the Haar wavelet with an increasing number of decomposition levels. In scenario 2, with the ascent in decomposition level, retained energy declined with the rise in the threshold.

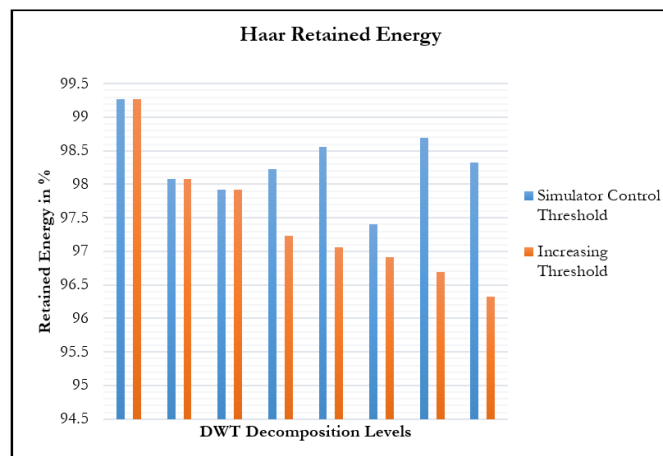


Figure 9: Trend of Haar retained energy.

Results on Symlets DWT Family:

The Symlets wavelets are known for their nearly symmetrical nature, which are modifications proposed by Daubechies to enhance symmetry while maintaining simplicity. Daubechie modifications aimed to increase the symmetry of wavelets while keeping them easy to use. The results of the Symlets (sym2) family using wavelets levels of decomposition up to 8 in scenario 1 are elaborated. When the DWT family is sym2 and the level increases from 1 to 3, the retained energy declines. At level 3, symlet2, the obtained energy was recorded as 98.08%. It represents that result at level 3 is low and increased retained energy was observed as shown in Figure 10. This symmetrical behavior is due to the nature of the symlets filter. In scenario 2, the loss in energy was observed with growth in decomposition level and threshold.

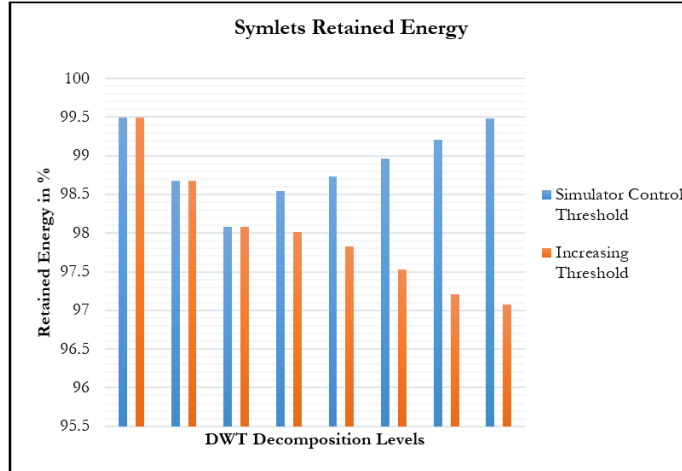


Figure 10: Trend of Symlets retained energy.

Coif lets DWT Family

Coif lets, derived from the Daubechies wavelet, exhibit higher symmetry and smoother wavelet characteristics compared to Daubechies mother wavelets. They are known for their increased computational overhead and utilize overlapping windows, enhancing their capabilities in various image processing techniques such as image denoising. For the family coif1 and the decomposition level 3 retained energy was 98.03%. There is a consistent drop from level 1 to 3, we have seen an increase and then a decline at levels 4 and 5. Again a symmetrical increase in retained energy was observed from decomposition level 5 to 8. This justifies the pattern of the Coif lets filter as shown in Figure 11 with the simulator control threshold. Whereas scenario 2 of the growing threshold with gain in decomposition levels, shows a decline in retained energy as shown in Figure 11 with increasing threshold.

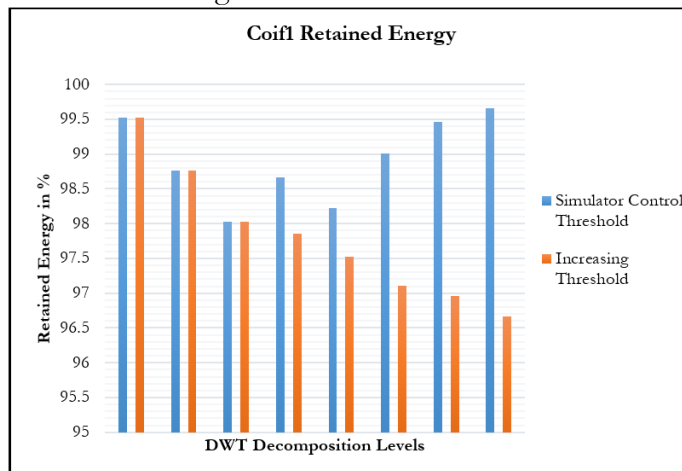


Figure 11: Trend of Coif lets retained energy.

Results on Bior Splines DWT Family:

The Bior Splines are biorthogonal spline functions with dense support, characterized by their symmetry and exact reconstruction properties. At level 3, the retained energy was 97.92% which shows the least value. However, there is an improvement in retained energy while upgrading to level 4, followed by a consistent behavior recorded from levels 5 to 8, as in Figure 12. These results were obtained using the Bior Splines filter where the threshold is taken by the simulator automatically and justifies the behavior of said filter in terms of retained energy. Additionally, in scenario 2, a decline in retained energy was recorded with increasing decomposition levels as in the increasing threshold of Figure 12.

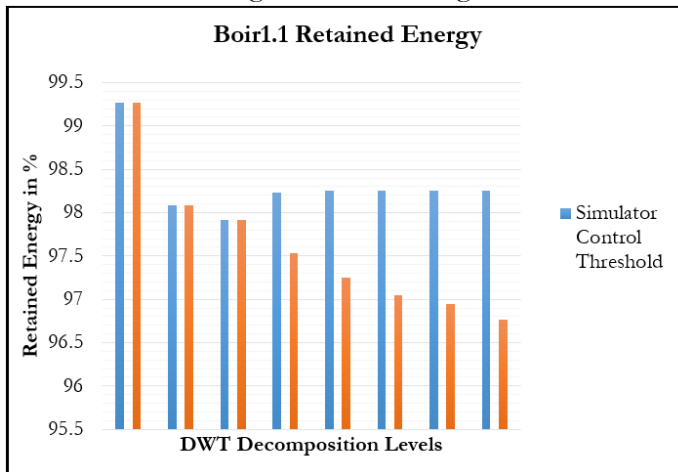


Figure 12: Trend of Bior Splines retained energy.

Results on Reverse Bior DWT Family:

The reverse Bior and Bior Spline share similar characteristics but the reconstruction and decomposition patterns are inverse of one another. The results of wavelets decomposition levels up to 8 and the Reverse Bior (rbio1.1) family in scenario 1 were evaluated. When the family is rbio1.1 and level is 3, retained energy was recorded as 97.92% which shows the lowest retained energy and results declined from level 1 to 3. The upgradation and constant behavior were observed in Figure 13 of the simulator control threshold. In scenario 2, for a greater threshold and highest decomposition level, the loss in retained energy is maximal, as illustrated in Figure 13 with the increasing threshold.

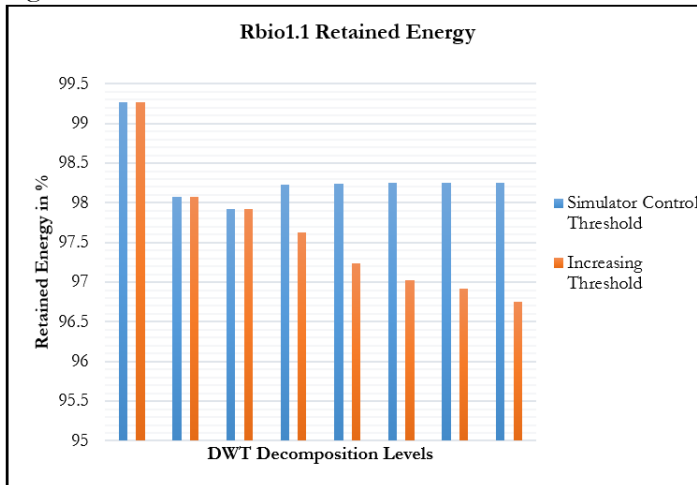


Figure 13: Trend of Reverse Bior retained energy.

DMeyer DWT Family:

The results of this family show that at level 5, the retained energy was recorded as 95.65%. The results of compression from decomposition level 1 to 5 degraded consistently. It

should be noted that except dmey all other DWT families showed consistent high to low results from de-composition level 1 to level 3. The graphical results of dmey for scenario 1 are shown in Figure 14. In scenario 2, with an increase in DWT levels, the energy retained by the DMeyer wavelet is decreasing showing inverse behavior as shown in Figure 14 of the increasing threshold.

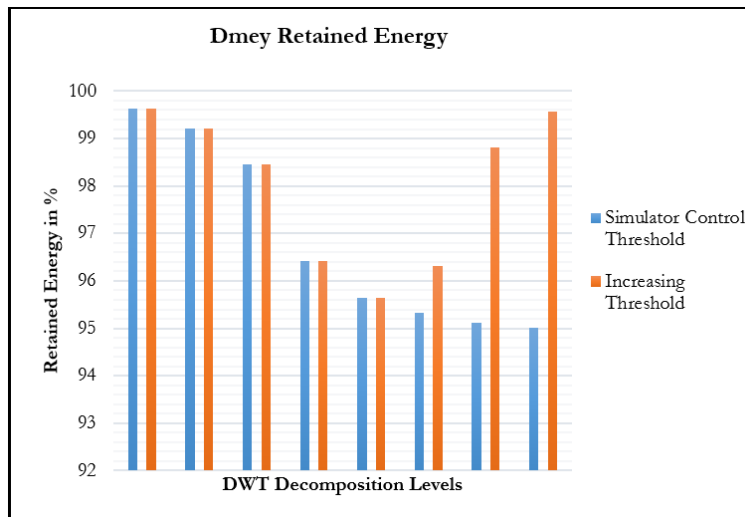


Figure 14: Trend of Dmey retained energy.

Discussion on Results:

As in wavelet analysis, images are represented by a set of basic functions. A single prototype function called the mother wavelet is used for deriving the basis function, by translating and dilating the mother wavelet. The wavelet transform can be viewed as a decomposition of an image in the time scale plane. In this work, Daubechies, Haar, Symlets, Coif lets, Bior Splines, Reverse Bior, DMeyer wavelets families, and decomposition levels up to 8 are used based on Equations 3, 5, and 6. For the overall results, we have taken two scenarios, scenario 1 has a simulator control threshold while scenario 2 has an increasing threshold with increasing decomposition levels of DWT. In scenario 1, different patterns of retained energy in wavelet families at various decomposition levels have been perceived. It is observed that in most families from level 1 to 3, retained energy is decreasing steadily leading to random behavior i.e., oscillating and non-oscillating in different families. As the retained energy is helpful in image compression, denoising, smoothing, and reconstruction, this work provides in a novel way, baseline results of various wavelet families with simulator control Birge– Massart thresholding strategy. It's crucial to evaluate results based on attributes like retained energy and compression ratio to understand the effectiveness of each wavelet filter family. This analysis helps in determining how well each filter performs according to its specific attributes and characteristics.

While scenario 2 shows that as the number of decomposition levels increases, the number of sets of detail level coefficients increases. For example, if four levels of decomposition are performed, one will obtain one set of level-4 approximation coefficients and four sets of detail-level coefficients for each level. The detail coefficients are thresholded, which requires setting some coefficients to zero. Specifically, the unnecessary high-frequency components that are present in the detail level coefficients for removal, while the necessary sharp changes (important discontinuous information) are retained. The coefficients with a magnitude less than the threshold are set to zero. The increase in thresholding with decomposition levels is an important consideration in image compression using wavelet transforms. Thus, the higher the decomposition level, the higher the number of coefficients will be set to zero, which will reduce the norm of the compressed wavelet coefficients vector and hence reduce the percent retained energy. Therefore, with increasing levels of decomposition, the threshold is also increasing,

which results increase in compression ratio and a decrease in retained energy. The relationship between retained energy and decomposition levels is inversely proportional in scenario 2. These findings can be used for various applications based on our needs. The proposed manipulations can be applied to images, including filtering, feature extraction, classification, and more. These manipulations are based on the results obtained from wavelet transform analysis. They help in selecting the most suitable form of wavelet transform for specific image processing tasks.

Selecting the appropriate decomposition level and wavelet function is crucial for accurately reconstructing the original signal and extracting desired features in image analysis. This decision plays a significant role in ensuring the effectiveness and precision of image-processing tasks. In this research, based on our needs and expectations we decided to choose the proper level of decomposition. Using this method, it is possible to have a thorough understanding of the characteristics of each decomposition. As much as the level of decomposition increases the retained energy i.e. responsible for image reconstruction after compression decreases to a certain level. So, the significance of this research is help to design a filter to eliminate noises i.e., to have a smooth image with no roughness via wavelet transform functions, we need to have an understanding of the frequency of probable noises and implement decomposition level properly to the frequency of noise, then we should discard noisy signals. Afterwards, the noise has been eliminated and the desired compressed signal is reconstructed. Thereby, we could have an efficient filter, while we keep the content of the image, we can reduce the effect of noise using this method.

Conclusion:

In a nutshell, it has been concluded that discrete wavelets transform definitely has an effect on the retained energy (RE) and Number of Zeros (NoZ) but the efficiency of DWT depends on the type of image, decomposition level, threshold, and also type/family of transform used. For the maximum value of the threshold and a higher level of decomposition, more energy is lost because, at upper levels of decomposition, there is a higher proportion of the coefficients in the detail sub-signals. Therefore, it is also necessary to select the finest value of the threshold to get minimum loss of images and achieve higher compression. The thresholding and wavelet families have central importance in terms of smoothness and closeness of fit. If the threshold is low, retained energy will be higher and the result will be close to the input, but this results in a low compression ratio. Whereas a large threshold produces a large number of zeros due to which output has smoothness it may cause blurs if it increases from a certain level.

Therefore, up to some specific level wavelet family and decomposition level synchronization produced the best results, and then degradation occurred due to loss of data and blurriness. These reference line manipulations help to choose the appropriate wavelet family and decomposition level according to the need for various applications of image compression. Image compression, utilizing wavelet transform brings about an improved ratio of compression, retained energy, and image quality. Wavelet change is the main technique that gives both spatial and frequency domain information. These properties of wavelet change help remarkably to identify and select important and non-essential coefficients among wavelet transform. From the comparative analysis of different transform schemes, it is deduced that currently, wavelet transforms give the most encouraging method to achieve superior image compression which is important for many real-world applications on the basis of thresholding, retained energy, number of zeroes, and compression ratio.

Acknowledgment: This work is supported by the Secured IoT Devices Lab, Department of Computer Systems Engineering, University of Engineering and Technology, Peshawar.

Funding: This research received no external funding.

Conflict of Interest: The authors declare no conflict of interest.

References:

- [1] V. A. Coutinho, R. J. Cintra, F. M. Bayer, P. A. M. Oliveira, R. S. Oliveira, and A. Madanayake, "Pruned Discrete Tchebichef Transform Approximation for Image Compression," *Circuits, Syst. Signal Process.*, vol. 37, no. 10, pp. 4363–4383, Oct. 2018, doi: 10.1007/S00034-018-0768-X/METRICS.
- [2] A. Sarwar, A. M. Alnajim, S. N. K. Marwat, S. Ahmed, S. Alyahya, and W. U. Khan, "Enhanced Anomaly Detection System for IoT Based on Improved Dynamic SBPSO," *Sensors* 2022, Vol. 22, Page 4926, vol. 22, no. 13, p. 4926, Jun. 2022, doi: 10.3390/S22134926.
- [3] S. Alyahya, W. U. Khan, S. Ahmed, S. N. K. Marwat, and S. Habib, "Cyber Secure Framework for Smart Agriculture: Robust and Tamper-Resistant Authentication Scheme for IoT Devices," *Electron.* 2022, Vol. 11, Page 963, vol. 11, no. 6, p. 963, Mar. 2022, doi: 10.3390/ELECTRONICS11060963.
- [4] I. Daubechies, M. Barlaud, and P. Mathieu, "Image Coding Using Wavelet Transform," *IEEE Trans. Image Process.*, vol. 1, no. 2, pp. 205–220, 1992, doi: 10.1109/83.136597.
- [5] A. Joseph, O. Okassa, J. P. Ngantcha, A. Ndtoungou, and P. Ele, "Use of Lazy Wavelet and DCT for Vibration Signal Compression," *Am. J. Eng. Appl. Sci.*, vol. 14, no. 1, pp. 1–6, Jan. 2021, doi: 10.3844/AJEASSP.2021.1.6.
- [6] R. Ranjan, "Canonical Huffman Coding Based Image Compression using Wavelet," *Wirel. Pers. Commun.*, vol. 117, no. 3, pp. 2193–2206, Apr. 2021, doi: 10.1007/S11277-020-07967-Y/METRICS.
- [7] R. Starosolski, "Employing New Hybrid Adaptive Wavelet-Based Transform and Histogram Packing to Improve JP3D Compression of Volumetric Medical Images," *Entropy* 2020, Vol. 22, Page 1385, vol. 22, no. 12, p. 1385, Dec. 2020, doi: 10.3390/E22121385.
- [8] M. A. Kabir and M. R. H. Mondal, "Edge-based and prediction-based transformations for lossless image compression," *J. Imaging*, vol. 4, no. 5, 2018, doi: 10.3390/JIMAGING4050064.
- [9] M. A. Rahman, M. Hamada, and J. Shin, "The Impact of State-of-the-Art Techniques for Lossless Still Image Compression," *Electron.* 2021, Vol. 10, Page 360, vol. 10, no. 3, p. 360, Feb. 2021, doi: 10.3390/ELECTRONICS10030360.
- [10] Z. Yin, W. Z. Shi, Z. Wu, and J. Zhang, "Multilevel wavelet-based hierarchical networks for image compressed sensing," *Pattern Recognit.*, vol. 129, p. 108758, Sep. 2022, doi: 10.1016/J.PATCOG.2022.108758.
- [11] S. Khan, S. Nazir, A. Hussain, A. Ali, and A. Ullah, "An efficient JPEG image compression based on Haar wavelet transform, discrete cosine transform, and run length encoding techniques for advanced manufacturing processes," *Meas. Control (United Kingdom)*, vol. 52, no. 9–10, pp. 1532–1544, Nov. 2019, doi: 10.1177/0020294019877508/ASSET/IMAGES/LARGE/10.1177_0020294019877508-FIG13.JPEG.
- [12] W. U. Khan, S. N. K. Marwat, and S. Ahmed, "Cyber Secure Framework for Smart Containers Based on Novel Hybrid DTLS Protocol," *Comput. Syst. Sci. Eng.*, vol. 43, no. 3, pp. 1297–1313, May 2022, doi: 10.32604/CSSE.2022.024018.
- [13] A. Kourav and A. Sharma, "Comparative analysis of wavelet transform algorithms for image compression," *Int. Conf. Commun. Signal Process. ICCSP 2014 - Proc.*, pp. 414–418, Nov. 2014, doi: 10.1109/ICCSP.2014.6949874.
- [14] A. Sarwar, S. Hasan, W. U. Khan, S. Ahmed, and S. N. K. Marwat, "Design of an Advance Intrusion Detection System for IoT Networks," *2nd IEEE Int. Conf. Artif. Intell. ICAI 2022*, pp. 46–51, 2022, doi: 10.1109/ICAI55435.2022.9773747.

- [15] C. Z. Basha, K. M. Sricharan, C. K. Dheeraj, and R. Ramya Sri, "A Study on Wavelet Transform Using Image Analysis," *Int. J. Eng. Technol.*, vol. 7, no. 2.32, pp. 94–96, May 2018, doi: 10.14419/IJET.V7I2.32.13535.
- [16] A. Maghari, "A comparative study of DCT and DWT image compression techniques combined with Huffman coding," *Jordanian J. Comput. Inf. Technol.*, vol. 5, no. 2, pp. 73–86, Aug. 2019, doi: 10.5455/JJCIT.71-1554982934.
- [17] D. Mody, P. Prajapati, P. Thaker, and N. Shah, "Image Compression Using DWT and Optimization Using Evolutionary Algorithm," *SSRN Electron. J.*, Apr. 2020, doi: 10.2139/SSRN.3568590.
- [18] S. P. Nanavati and P. K. Panigrahi, "Wavelets: Applications to image compression-I," *Reson.* 2005 102, vol. 10, no. 2, pp. 52–61, Feb. 2005, doi: 10.1007/BF02835922.
- [19] S. Sidhik, "Comparative study of Birge–Massart strategy and unimodal thresholding for image compression using wavelet transform," *Optik (Stuttg.)*, vol. 126, no. 24, pp. 5952–5955, Dec. 2015, doi: 10.1016/J.IJLEO.2015.08.127.
- [20] M. Rabbani and R. Joshi, "An overview of the JPEG 2000 still image compression standard," *Signal Process. Image Commun.*, vol. 17, no. 1, pp. 3–48, Jan. 2002, doi: 10.1016/S0923-5965(01)00024-8.
- [21] M. A. Rahman and M. Hamada, "Lossless Image Compression Techniques: A State-of-the-Art Survey," *Symmetry* 2019, Vol. 11, Page 1274, vol. 11, no. 10, p. 1274, Oct. 2019, doi: 10.3390/SYM11101274.
- [22] J. A. Aghamaleki and A. Ghorbani, "Image fusion using dual tree discrete wavelet transform and weights optimization," *Vis. Comput.*, vol. 39, no. 3, pp. 1181–1191, Mar. 2023, doi: 10.1007/S00371-021-02396-9/METRICS.
- [23] J. Ma, J. Jiang, C. Liu, and Y. Li, "Feature guided Gaussian mixture model with semi-supervised EM and local geometric constraint for retinal image registration," *Inf. Sci. (Ny)*, vol. 417, pp. 128–142, Nov. 2017, doi: 10.1016/J.INS.2017.07.010.
- [24] M. C. Yesilli, J. Chen, F. A. Khasawneh, and Y. Guo, "Automated surface texture analysis via Discrete Cosine Transform and Discrete Wavelet Transform," *Precis. Eng.*, vol. 77, pp. 141–152, Sep. 2022, doi: 10.1016/J.PRECISIONENG.2022.05.006.



Copyright © by authors and 50Sea. This work is licensed under Creative Commons Attribution 4.0 International License.